have observed that glow discharges without cathode-fall are obtained with cathodes made of semi-conductors covered with a thin layer of insulating material. Metal cathodes covered in the same way have a cathode fall but the discharge is accompanied by small sparks on the cathode surface. In a similar way insulating layers formed chemically on the cathode surfaces in the experiments described might give rise to the flashes observed at large currents.

The perfectly smooth surfaces of the cathode spots in air and oxygen and the restlessness of the negative glow in nitrogen are direct evidences of complicated phenomena on the cathode surface. More definite statements about the chemical effects cannot be made, however, until the disturbances have been studied under very pure conditions.

APRIL 15, 1939 PHYSICAL REVIEW VOLUME 55

A Dynamic Measurement of the Elastic, Electric and Piezoelectric Constants of Rochelle Salt

W. P. MASON
Bell Telephone Laboratories, New York, New York

(Received November 12, 1938)

The elastic, electric and piezoelectric constants of Rochelle salt have been measured at low field strengths by measuring the resonant frequencies and impedance of vibrating crystals. It is shown experimentally that the resonant and antiresonant frequencies of the crystal are both considerably below the natural mechanical resonant frequency of the crystal in disagreement with the usual derivation of the frequencies of a piezoelectric crystal. By assuming that the piezoelectric stress is proportional to the charge density on the electrodes rather than the potential gradient as usually assumed, theoretical frequencies are obtained which agree with those found experimentally. This theoretical derivation together with the measured frequencies supply values for the piezoelectric constants. The elastic constants measured dynamically show some differences from those measured statically. A large difference is found for the dynamically measured piezoelectric constants from those statically measured, which may be attributed to the finite relaxation time for the piezoelectric elements.

I. INTRODUCTION

THE static properties of Rochelle salt crystals have formed the subject for a number of measurements. W. Mandell[1] has measured the nine elastic constants of Rochelle salt by a static method, and a number of measurements have been made on the dielectric constants and the piezoelectric constants. However, very few measurements[2] have been made on the dynamic characteristics of Rochelle salt, which may differ considerably from the static characteristics due principally to the large relaxation time of the piezoelectric elements of the crystal. It is the purpose of this paper to present dynamic measurements on the elastic, dielectric and piezoelectric constants of Rochelle salt crystals. These indicate a considerable difference from those determined statically, particularly the piezoelectric and the dielectric constants. Because of the precision obtainable in frequency determination it is felt that the measurements made in this way should be more accurate than those obtained by other methods.

In measuring the elastic constants of a crystal, the frequency of resonance of some known mode of motion is measured electrically and the elastic constant is calculated from this measurement and the known density of the crystal. The usual method of deriving the equations of motion[3]

[1] "The Determination of the Elastic Modulii of the Piezo-Electric Crystal Rochelle Salt by a Statical Method," W. Mandell, Proc. Roy. Soc. London **116**, 623 (1927).

[2] One of the dynamic piezoelectric constants was recently measured by G. Mikhailov (Tech. Phys. U. S. S. R. **4**, 461 (1937)) using a different method. He does not obtain as high a piezoelectric constant as measured by this method.

[3] See for example *Quartz Resonators and Oscillators*, P. Vigoureux (H.M. Stationery Office, London), Chapter III, or *Piezo-electrizitat Des Quarzes*, Adolf Schiebe (Theodor Steinkopff, 1938), p. 85.

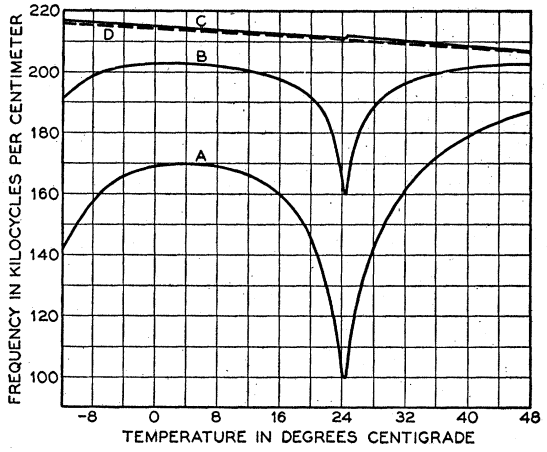

FIG. 1. Measured frequencies for a longitudinally vibrating Rochelle salt crystal measured as a function of the temperature. Curves *A* and *B* are, respectively, the measured resonance and antiresonance frequencies of a fully plated crystal. Curve *C* is the measured resonance (or antiresonance) frequency of a crystal lightly plated at the center or an unplated crystal in an air-gap holder. Curve *D* the calculated natural mechanical resonance of the fully plated crystal.

(which is based on the assumed proportionality between piezoelectric stress and applied potential gradient in the crystal) indicates that the resonant frequency of the crystal measured electrically coincides with the natural mechanical resonance of the crystal.[4] As is evident from a measurement of the resonant and antiresonant frequencies of a highly coupled crystal such as Rochelle salt, this deduction does not agree with experiment. The data on Fig. 1 show measured resonance curves for a longitudinally vibrating Rochelle salt crystal with its major surfaces perpendicular to the *a* or electric axis of the crystal, and the length of the crystal laying 45° from the *b* and *c* axes. The curves labeled *A* and *B* are, respectively, the electrical resonant frequencies (frequencies of smallest impedance) and the electrical antiresonant frequencies (frequencies of largest impedance) of a fully plated crystal plotted as a function of the temperature of the crystal. The dimensions of the crystal—which were chosen so that no secondary resonances were present near the main one—were length = 2.014 cm; width = 0.418 cm; thickness = 0.104 cm; and the measured frequencies were expressed in terms of a crystal one centimeter long. The curve labeled *C* is a measurement of the resonant frequency (or antiresonant frequency since the two are nearly identical) of the same crystal with the plating removed except for a small amount at the center. The curve *C* is also obtained for an unplated crystal in an air-gap holder with a large air gap. As is evident the curve *C* is considerably higher in frequency than either *A* or *B*.

If we assume that the piezoelectric stress is proportional to the applied field, it is evident that the curves *A* and *C* should be identical, for the piezoelectric driving force will be in phase with the applied potential irrespective of the amount of the crystal plated and hence in both cases the resonant frequency measured should agree with the natural mechanical resonant frequency of the crystal, a deduction that does not agree with experiment.

This question is considered in Appendix II and it is there shown that if the piezoelectric stress is taken proportional to the charge density on the electrodes, resonant and antiresonant frequencies are obtained which agree with the experimental results. From these theoretical results and the measured frequencies of Fig. 1, one of the piezoelectric constants of the crystal can be evaluated. It is shown also in Appendix II that if the driving plates and the crystal are separated by a large air gap, the electrical resonant and antiresonant frequencies coincide with the natural mechanical resonant frequency of the crystal and hence by measuring the electrical frequencies of the crystal in an air-gap holder, the true elastic constants of the crystal can be evaluated.

II. Measurements of the Nine Elastic Constants of Rochelle Salt

Rochelle salt belongs to the rhombic hemihedral class of crystals and possess three diagonal axes of symmetry which are identical with the three crystallographic axes. As a consequence of its class of symmetry it has nine elastic constants, and three piezoelectric constants all of which are shears for the three crystallographic axes.

If we associate the *a* axis with an *X* axis, the *b* axis with a *Y* axis, and the *c* with a *Z* axis, the

[4] For a plated crystal this deduction is obvious since for a plated crystal the applied potential is constant along the surface and hence the applied piezoelectric forces cancel out everywhere except at the two ends. The applied mechanical force on the ends of the crystal will be in phase with the applied potential and hence the electrical and mechanical resonances will occur at the same frequency.

elastic equations for a Rochelle salt crystal are

$$\begin{aligned} -x_x &= s_{11}X_x + s_{12}Y_y + s_{13}Z_z; \quad -y_z = s_{44}Y_z, \\ -y_y &= s_{12}X_x + s_{22}Y_y + s_{23}Z_z; \quad -z_x = s_{55}Z_x, \\ -z_z &= s_{13}X_x + s_{23}Y_y + s_{33}Z_z; \quad -x_y = s_{66}X_y, \end{aligned} \tag{1}$$

in which s_{11} etc. are the nine elastic compliances, x_x etc. the strains, and X_x etc. the stresses. We may also write this relationship in the form

$$\begin{aligned} -X_x &= c_{11}x_x + c_{12}y_y + c_{13}z_z; \quad -Y_z = c_{44}y_z, \\ -Y_y &= c_{12}x_x + c_{22}y_y + c_{23}z_z; \quad -Z_x = c_{55}z_x, \\ -Z_z &= c_{13}x_x + c_{23}y_y + c_{33}z_z; \quad -X_y = c_{66}x_y, \end{aligned} \tag{1'}$$

where

$$\sigma c_{11} = \begin{vmatrix} s_{22}s_{23} \\ s_{23}s_{33} \end{vmatrix}; \quad \sigma c_{23} = \begin{vmatrix} s_{13}s_{23} \\ s_{11}s_{12} \end{vmatrix};$$

$$c_{44} = \frac{1}{s_{44}} \quad \text{where} \quad \sigma = \begin{vmatrix} s_{11}s_{12}s_{13} \\ s_{12}s_{22}s_{23} \\ s_{13}s_{23}s_{33} \end{vmatrix}.$$

The simplest way to measure the modulii of compliance s_{11}, s_{22}, s_{33} (which are the inverse of Young's modulii along the X, Y and Z axes) is to cut crystals having their lengths large compared to any other dimensions, and lying respectively along the X, Y and Z axes, then to measure the frequencies of resonance of such crystals. The value of the modulus of compliance is obtained from the formula

$$f = \frac{1}{2l}\left(\frac{1}{\rho s_{nn}}\right)^{\frac{1}{2}} \quad \text{or} \quad s_{nn} = \frac{1}{(2lf)^2\rho}, \tag{2}$$

where l is the length of the crystal, f is the frequency of mechanical resonance, and ρ the density of Rochelle salt which after careful measurement[5] was found to be

$$\rho = 1.775. \tag{3}$$

Unfortunately, however, crystals cut along these three axes have no components of driving force to drive them in a longitudinal mode. However, if the crystal is cut at an angle to any of the three axes, the piezoelectric constant determining the longitudinal driving force is finite as shown in Appendix I, and a measurable resonance is obtained. Accordingly crystals were cut with their thin dimensions perpendicular to the X, Y and Z axes, respectively, with their long dimensions at various angles from the other crystallographic axes. These crystals and their frequencies measured in an air-gap holder are given on Table I. The frequencies were all measured at 30°C.

TABLE I.

(1) Direction of Applied Potential	(2) Angle From	(3) Dimensions in mm L	W	T	(4) Frequency of Resonance Cycles	(5) Frequency Constant kc per cm	(6) Value of s Constants
1 X	Y =22.5°	20.02	2.14	1.08	102,420	204.9	3.36×10^{-12}
2 X	Y =45°	20.22	2.24	.98	104,110	210.5	3.16
3 X	Y =67.5°	19.72	2.26	1.06	105,670	208.4	3.23
4 Y	X =67.5°	19.86	2.16	1.06	76,340	151.6	6.14
5 Y	X =45°	20.06	2.08	1.02	61,176	122.7	9.31
6 Y	X =22.5°	19.94	2.14	.98	68,820	137.25	7.45
7 Z	X =67.5°	19.84	2.08	.96	100,810	200.0	3.525
8 Z	X =45°	19.65	2.12	.98	96,570	189.9	3.905
9 Z	X =22.5°	19.42	2.12	.98	89,320	173.2	4.69

Unfortunately, however, crystals cut along these three axes have no components of driving force to drive them in a longitudinal mode. However, if the crystal is cut at an angle to any of the three axes, the piezoelectric constant determining the longitudinal driving force is finite as shown in Appendix I, and a measurable resonance is obtained. Accordingly crystals were cut with their thin dimensions perpendicular to the X, Y and Z axes, respectively, with their long dimensions at various angles from the other crystallographic axes. These crystals and their frequencies measured in an air-gap holder are given on Table I. The frequencies were all measured at 30°C.

In order to use these values it is necessary to know how Young's modulus varies for different angular cuts. The variation with orientation is worked out in Appendix I. For a crystal cut perpendicular to the a or X axis this becomes

$$s_{22}' = s_{22}\cos^4\theta + (2s_{23}+s_{44})\sin^2\theta\cos^2\theta + s_{33}\sin^4\theta, \tag{4}$$

where θ is the angle between the long dimension and the Y axis. The value of s_{22}' is given for three angles by the first three values of column 6, and hence the three unknown quantities s_{22}, $(2s_{23}+s_{44})$ and s_{33} can be solved for. We find

$$\begin{aligned} s_{22} &= 3.50\times10^{-12}; \quad s_{33} = 3.32\times10^{-12}; \\ (2s_{23}+s_{44}) &= 5.93\times10^{-12}. \end{aligned} \tag{5}$$

For a rotation about the Y axis the expression for s_{11}' becomes

$$s_{11}' = s_{11}\cos^4\theta + (2s_{13}+s_{55})\sin^2\theta\cos^2\theta + s_{33}\sin^4\theta, \tag{6}$$

where θ is the angle measured from the X axis. The data for crystals 4, 5 and 6 are applicable to this case, and we find

$$\begin{aligned} s_{11} &= 5.23\times10^{-12}; \quad s_{33} = 3.365\times10^{-12}; \\ (2s_{13}+s_{55}) &= 28.6\times10^{-12}. \end{aligned} \tag{7}$$

[5] This measurement was made by Mr. W. L. Bond.

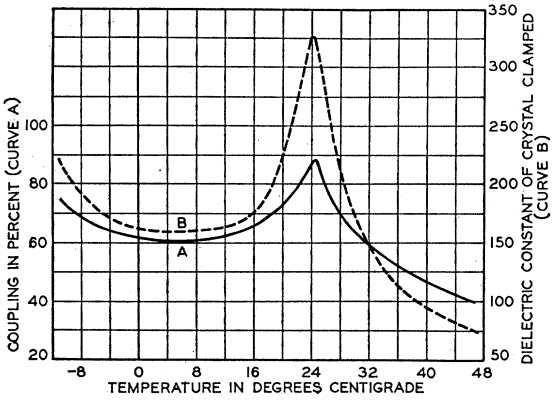

FIG. 2. Dynamic electric and coupling constants of an X cut Rochelle salt crystal. Curve A represents the electromechanical coupling of the crystal. Curve B represents the dielectric constant of the crystal clamped, plotted as a function of the temperature.

Similarly for a rotation about Z we find

$$s_{11}'=s_{11}\cos^4\theta+(2s_{12}+s_{66})\sin^2\theta\cos^2\theta+s_{22}\sin^4\theta \quad (8)$$

and from the data for crystals 7, 8 and 9 we find

$$s_{11}=5.14\times10^{-12};\quad s_{22}=3.495\times10^{-12};\quad (2s_{12}+s_{66})=7.02\times10^{-12}. \quad (9)$$

There are two independent values for s_{11}, s_{22} and s_{33} and a comparison shows that they agree within about one percent, which is the order of accuracy of the measurement. By these measurements we have evaluated three constants, and have three relations between the remaining six constants.

In order to evaluate the remaining constants it is necessary to measure the three shear coefficients s_{44}, s_{55}, s_{66}. It is shown in Appendix I, that if a crystal is cut with one edge of its major surface lying along one of the crystallographic axes and the normal to the major surface at an angle between the other two crystallographic axes, a piezoelectric constant results which sets up a high frequency shear wave in the crystal similar to the high frequency shear vibration excited in Y or AT cut quartz. The resonances of a large thin plate have been worked out by E. B. Christofel[6] who showed that there were three different values whose velocity of propagation could be obtained from the determinant

$$\begin{vmatrix}\lambda_{11}-\rho v^2, & \lambda_{12}, & \lambda_{13}\\ \lambda_{12}, & \lambda_{22}-\rho v^2, & \lambda_{23}\\ \lambda_{13}, & \lambda_{23}, & \lambda_{33}-\rho v^2\end{vmatrix}=0. \quad (10)$$

In this equation ρ is the density, v the velocity of propagation, and the λ's are related to the elastic constants of the crystal by the formulae

$$\begin{aligned}
\lambda_{11}&=c_{11}l^2+c_{66}m^2+c_{55}n^2+2c_{56}mn+2c_{15}nl+2c_{16}lm,\\
\lambda_{22}&=c_{66}l^2+c_{22}m^2+c_{44}n^2+2c_{23}mn+2c_{46}nl+2c_{26}lm,\\
\lambda_{33}&=c_{55}l^2+c_{44}m^2+c_{33}n^2+2c_{34}mn+2c_{35}nl+2c_{45}lm,\\
\lambda_{12}&=c_{16}l^2+c_{26}m^2+c_{45}n^2+(c_{46}+c_{25})mn+(c_{14}+c_{56})nl+(c_{12}+c_{66})lm,\\
\lambda_{13}&=c_{15}l^2+c_{46}m^2+c_{35}n^2+(c_{45}+c_{36})mn+(c_{13}+c_{55})nl+(c_{14}+c_{56})lm,\\
\lambda_{23}&=c_{56}l^2+c_{24}m^2+c_{34}n^2+(c_{44}+c_{25})mn+(c_{36}+c_{45})nl+(c_{25}+c_{46})lm,
\end{aligned} \quad (11)$$

where l, m and n are, respectively, the direction cosines between the normal to the surface which is the direction of propagation and the X, Y and Z axes. For Rochelle salt

$$c_{14}=c_{15}=c_{16}=c_{24}=c_{25}=c_{26}=c_{34}=c_{35}=c_{36}=c_{45}=c_{46}=c_{56}=0.$$

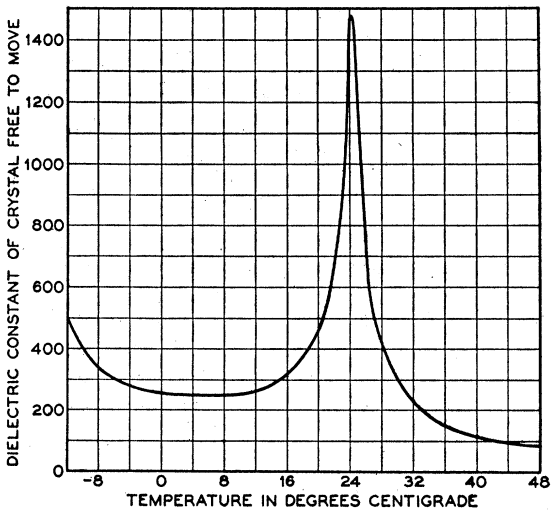

FIG. 3. Dielectric constant of an X cut Rochelle salt crystal free to move plotted as a function of the temperature.

[6] See A. E. H. Love's *Theory of Elasticity* (Cambridge University Press, 1934), fourth edition, p. 298.

For a crystal one edge of which lies along the X axis and the normal to the surface makes an angle θ with the Y axis $l=0$, $m=\cos\theta$, $n=\sin\theta$. Hence we find that

$$\begin{aligned}&\lambda_{11}=c_{66}\cos^2\theta+c_{55}\sin^2\theta;\quad \lambda_{12}=\lambda_{13}=0;\\&\lambda_{23}=(c_{25}+c_{44})\sin\theta\cos\theta;\\&\lambda_{22}=c_{22}\cos^2\theta+c_{44}\sin^2\theta;\\&\lambda_{33}=c_{44}\cos^2\theta+c_{33}\sin^2\theta.\end{aligned}\tag{12}$$

Since λ_{12} and λ_{13} are zero we have a shear mode of motion whose velocity is given by

$$v=(\lambda_{11}/\rho)^{\frac{1}{2}}$$ and whose frequency by

$$f=\frac{1}{2l_t}\left(\frac{c_{66}\cos^2\theta+c_{55}\sin^2\theta}{\rho}\right)^{\frac{1}{2}}.\tag{13}$$

Similarly for a crystal with one edge lying along the Y axis and the normal to the surface making an angle θ with the Z axis, we have a shear mode given by

$$f=\frac{1}{2l_t}\left(\frac{c_{44}\sin^2\theta+c_{66}\cos^2\theta}{\rho}\right)^{\frac{1}{2}}.\tag{14}$$

For a crystal lying along Z and whose normal makes an angle θ with the Y axis the frequency of resonance becomes

$$f=\frac{1}{2l_t}\left(\frac{c_{55}\cos^2\theta+c_{44}\sin^2\theta}{\rho}\right)^{\frac{1}{2}}.\tag{15}$$

These shear modes are the ones driven by the piezoelectric constants of the crystal.

In order to determine the constants c_{44}, c_{55} and c_{66} eight crystals were cut as shown on Table II and their resonant frequencies measured.

TABLE II.

Edge lies along	Angle of Normal from	Dimensions in mm L	W	T	Frequency Constant kc per mm	Value of c constant	No. of Crystal
X	22.5° from Y	19.98	19.98	2.05	1129	7.51×10^{10}	1
X	45° from Y	29.24	29.24	1.92	945.2	6.34×10^{10}	2
X	67.5° from Y	24.00	23.98	2.36	755	4.06×10^{10}	3
Y	22.5° from X	25.44	25.44	2.28	1197	10.18×10^{10}	4
Y	45° from X	26.58	26.59	1.37	1265	11.39×10^{10}	5
Y	67.5° from X	20.66	20.64	1.72	1299	11.99×10^{10}	6
Z	22.5° from X	25.44	25.46	2.06	799.2	4.54×10^{10}	7
Z	45° from X	27.56	27.54	2.26	1052.0	7.87×10^{10}	8

Solving for c_{55} and c_{66} using the first three crystals of this table and Eq. (13) we have

$$c_{55}=2.96\times10^{10};\quad c_{66}=10.02\times10^{10}.$$

Using Eq. (14) and crystals 4, 5 and 6, we find

$$c_{44}=12.43\times10^{10};\quad c_{66}=9.91\times10^{10}.$$

Using Eq. (15) and crystals 7 and 8, we find

$$c_{44}=12.61\times10^{10};\quad c_{55}=3.13\times10^{10}.$$

Averaging these results we have for the three shear coefficients

$$\begin{aligned}&c_{44}=12.52\times10^{10};\quad s_{44}=1/c_{44}=7.98\times10^{-12};\\&c_{55}=3.04\times10^{10};\quad s_{55}=1/c_{55}=32.8\times10^{-12};\\&c_{66}=9.96\times10^{10};\quad s_{66}=1/c_{66}=10.08\times10^{-12}.\end{aligned}$$

Inserting these values in the relations given previously we find for the nine elastic constants the results shown on Table III. These are compared with the static results obtained by Mandell.

III. Measurements of Dielectric, Coupling and Piezoelectric Constants of Rochelle Salt

The three piezoelectric constants and the three dielectric constants along the three crystallographic axes have been measured by measuring the resonances and the capacitances of crystals cut with their major surfaces perpendicular to these three axes. This work was done at field strengths below 40 volts per centimeter, where

TABLE III.

	s_{11}	s_{22}	s_{33}	s_{44}	s_{55}	s_{66}	s_{12}	s_{13}	s_{23}
Coefficient by Dynamic Method	5.18×10^{-12}	3.495	3.34	7.98	32.8	10.08	−1.53	−2.11	−1.03
Coefficient Measured by Mandell	4.69×10^{-12}	3.205	2.815	6.06	30.6	8.02	− .795	−2.18	+1.69

	c_{11}	c_{22}	c_{33}	c_{44}	c_{55}	c_{66}	c_{12}	c_{13}	c_{23}
Coefficient by Dynamic Method	42.5×10^{10}	51.5	62.9	12.52	3.04	9.96	+29.6	+35.7	+34.25
Coefficient Measured by Mandell	34.7×10^{10}	47.3	80.6	16.35	3.24	12.42	− 8.05	+31.6	−34.4

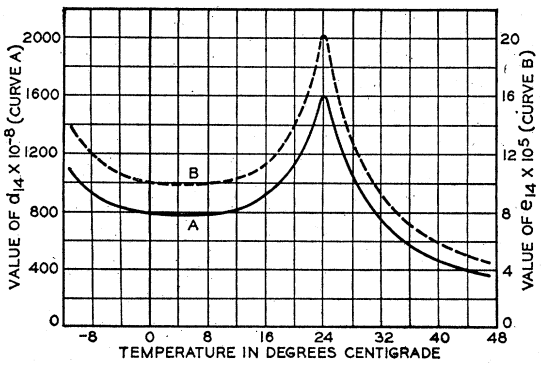

FIG. 4. Dynamic piezoelectric modulii of X cut Rochelle salt. Curve A is the piezoelectric constant d_{14} while curve B is the piezoelectric constant e_{14} plotted as a function of the temperature.

the expansion is a linear function of the applied field. The frequencies used were in the order of 80 kilocycles. Since it has been shown previously[7] that the constants are nearly independent of the frequency, above 100 cycles, the results can be used at other frequencies.

Figure 1 shows the measured resonance and antiresonance frequency of an X cut crystal with its length lying 45° from the Y and Z axes. With the aid of Fig. 7 of Appendix II, the electromechanical coupling defined by the Eq. (54) of Appendix II

$$k_x=\frac{d_{14}}{2}\left(\frac{4\pi}{Ks_{22}'}\right)^{\frac{1}{2}} \tag{17}$$

can be evaluated as a function of temperature and is plotted on Fig. 2, curve A. In Eq. (17) d_{14} is the piezoelectric constant, s_{22}' the inverse of Young's modulus along the length of the crystal and K the dielectric constant of the crystal when it is clamped or prevented from moving. In order to evaluate the piezoelectric constant d_{14} it is necessary to know the dielectric constant K. In order to determine this constant crystals were cut small enough to have no resonance near the frequency region of the resonances of the crystal of Fig. 1. The capacitance of the crystal free to vibrate was then measured over a temperature range and the dielectric constant resulting is shown on Fig. 3. It is shown in Appendix II, that the clamped dielectric constant is equal to the free dielectric constant divided by $(1-k^2)$. Hence from the data on Figs. 2 and 3 the dielectric constant K can be evaluated and it is plotted as curve B of Fig. 2. The value of s_{22}' for this crystal over a temperature range can be calculated from curve C of Fig. 1, hence from Eq. (17) the value of d_{14} can be evaluated and is shown as curve A of Fig. 4. Another piezoelectric constant e_{14} is sometimes used. This is related to d_{14} by

$$d_{14}/s_{44}=e_{14}. \tag{18}$$

The value of e_{14} is plotted as curve B of Fig. 4. The value of the piezoelectric constant obtained this way is smaller than that obtained statically, and moreover it shows a maximum at the Curie transformation point. Apparently the difference is due to the finite time of relaxation of the piezoelectric elements which do not allow them to attain their static value for an applied alternating voltage.

The values of the piezoelectric and dielectric constants along the other two axes were also measured and were found not to vary much with temperature. At 30°C, the Y constants were found to be

$$k_y=0.279;\quad K_y=12.5;\quad d_{25}=169\times10^{-8};\quad e_{25}=d_{25}/s_{55}=5.15\times10^4. \tag{19}$$

For the Z axis the results were

$$k_z=0.111;\quad K_z=10.2;\quad d_{36}=39.4\times10^{-8};\quad e_{36}=d_{36}/s_{66}=3.91\times10^4. \tag{20}$$

It will be noted that a dynamic method does not determine the sign of the piezoelectric constant but only its magnitude. From static measurements d_{25} is of opposite sign to d_{14} and d_{36}.

APPENDIX I

Constants of rotated rochelle salt crystals

The elastic equations of a Rochelle salt crystal are given by Eqs. (1) and (1′) when the a axis of the crystal is designated the X axis, the b the Y axis and the c the Z axis. The direct piezoelectric equations are

$$\begin{aligned} &P_x=d_{14}Y_z; \quad P_y=d_{25}Z_x; \quad P_z=d_{36}X_y,\\ &-P_x=e_{14}y_z; \quad -P_y=e_{25}z_x; \quad -P_z=e_{36}x_y, \end{aligned} \tag{21}$$

where P_x, P_y, P_z are the polarizations (charge per

[7] O. Norgorden, Phys. Rev. **49**, 820 (1936).

unit area) along the X, Y and Z axes, respectively. The usual method of writing the converse piezoelectric equations is

$$\begin{aligned} -Y_z&=e_{14}E_x; \quad -Z_x=e_{25}E_y; \quad -X_y=e_{36}E_z,\\ y_z&=d_{14}E_x; \quad z_x=d_{25}E_y; \quad x_y=d_{36}E_z, \end{aligned} \tag{22}$$

where E_x, E_y, E_z are the potential gradients along the X, Y and Z axes.

In determining the constants of the crystal it is desirable to obtain cuts along other directions than the three crystallographic axes and it is desirable to obtain the elastic and piezoelectric constants for these other cuts. These cuts are determined by a new set of axes X', Y', Z' related to the old crystallographic axes by the direction cosines l_1 to n_3 expressed by the equation

$$\begin{array}{cccc} & X & Y & Z \\ X' & l_1 & m_1 & n_1 \\ Y' & l_2 & m_2 & n_2 \\ Z' & l_3 & m_3 & n_3. \end{array} \tag{23}$$

The transformations of stress as given by Love[8] are

$$\begin{aligned} X_x'&=l_1^2X_x+m_1^2Y_y+n_1^2Z_z+2m_1n_1Y_z\\ &\quad+2n_1l_1Z_x+2l_1m_1X_y\\ &\cdots\cdots\cdots\cdots\\ X_y'&=l_1l_2X_x+m_1m_2Y_y+n_1n_2Z_z\\ &\quad+(m_1n_2+n_1m_2)Y_z\\ &\quad+(n_1l_2+n_2l_1)Z_x+(l_1m_2+l_2m_1)X_y, \end{aligned} \tag{24}$$

where the primes denote the stresses referred to the new axes. Conversely we have

$$\begin{aligned} X_x&=l_1^2X_x'+l_2^2Y_y'+l_3^2Z_z'+2l_2l_3Y_z'\\ &\quad+2l_3l_1Z_x'+2l_1l_2X_y'\\ &\cdots\cdots\cdots\cdots\\ X_y&=l_1m_1X_x'+l_2m_2Y_y'+l_3m_3Z_z'\\ &\quad+(l_2m_3+l_3m_2)Y_z'+(l_3m_1+l_1m_3)Z_x'\\ &\quad+(l_1m_2+l_2m_1)X_y'. \end{aligned} \tag{25}$$

Similarly the transformation for the strain becomes[9]

$$\begin{aligned} x_x'&=l_1^2x_x+m_1^2y_y+n_1^2z_z+m_1n_1y_z\\ &\quad+n_1l_1z_x+l_1n_1x_y\\ &\cdots\cdots\cdots\cdots\\ x_y'&=2l_1l_2x_x+2m_1m_2y_y+2n_1n_2z_z\\ &\quad+(m_1n_2+m_2n_1)y_z+(n_1l_2+n_2l_1)z_x\\ &\quad+(l_1m_2+l_2m_1)x_y \end{aligned} \tag{26}$$

[8] Reference 6, p. 80.
[9] Reference 6, p. 42.

and conversely

$$\begin{aligned} x_x&=l_1^2x_x'+l_2^2y_y'+l_3^2z_z'+l_2l_3y_z'\\ &\quad+l_3l_1z_x'+l_1l_2x_y'\\ &\cdots\cdots\cdots\cdots\\ x_y&=2l_1m_1x_x'+2l_2m_2y_y'+2l_3m_3z_z'\\ &\quad+(l_2m_3+l_3m_2)y_z'+(l_3m_1+l_1m_3)z_x'\\ &\quad+(l_1m_2+l_2m_1)x_y'. \end{aligned} \tag{27}$$

Polarization, being a vector, transforms according to the equations

$$\left.\begin{aligned} P_x&=l_1P_x'+l_2P_y'+l_3P_z',\\ P_y&=m_1P_x'+m_2P_y'+m_3P_z',\\ P_z&=n_1P_x'+n_2P_y'+n_3P_z', \end{aligned}\right\} \tag{28}$$

and conversely

$$\left.\begin{aligned} P_x'&=l_1P_x+m_1P_y+n_1P_z,\\ P_y'&=l_2P_x+m_2P_y+n_2P_z,\\ P_z'&=l_3P_x+m_3P_y+n_3P_z. \end{aligned}\right\}$$

We now consider the simple case of a section whose X axis remains unchanged but whose other axes are rotated by an angle θ with respect to the crystallographic axes. For this case

$$\begin{aligned} l_1&=1; \quad m_2=n_3=\cos\theta; \quad n_2=-m_3=\sin\theta;\\ l_2&=l_3=m_1=n_1=0. \end{aligned} \tag{29}$$

Then to determine the piezoelectric constants for a section of this kind we have

$$\begin{aligned} P_x'&=P_x=e_{14}y_z\\ &=e_{14}(y_y'\sin 2\theta-z_z'\sin 2\theta+y_z'\cos 2\theta). \end{aligned} \tag{30}$$

In the rotated crystal this would give a constant e_{12}' relating an expansion along the Y' axis with the X' polarization equal to $e_{14}\sin 2\theta$. Working out the polarization along the other two axes we find the constants

$$\begin{aligned} e_{12}'&=e_{14}\sin 2\theta; \quad e_{13}'=-e_{14}\sin 2\theta;\\ e_{14}'&=e_{14}\cos 2\theta;\\ e_{25}'&=[e_{25}\cos^2\theta-e_{36}\sin^2\theta];\\ e_{26}'&=(e_{25}+e_{36})\sin\theta\cos\theta;\\ e_{35}'&=-(e_{25}+e_{36})\sin\theta\cos\theta;\\ e_{36}'&=e_{36}\cos^2\theta-e_{25}\sin^2\theta. \end{aligned} \tag{31}$$

These equations show that for a crystal cut perpendicular to the X axis and with the length at an angle between the Y and Z axes a longitudinal vibration can be set up by the constant e_{12}' or e_{13}'. This vibration will have its maximum driving force when $\theta=45°$. These equations show also that if one axis of the principal plane lies along X and the normal to the principal plane makes an angle θ with the Y crystallographic axis, a high frequency shearing mode is set up by the constant e_{26}' and this reaches its maximum when $\theta=45°$.

The d constants transform similarly to the e constants, except for d_{12}' and d_{13}' which are equal to

$$d_{12}'=\tfrac{1}{2}d_{14}\sin 2\theta; \quad d_{13}'=-\tfrac{1}{2}d_{14}\sin 2\theta. \quad (32)$$

If we express the elastic equations for the rotated axes it is readily shown that

$$\begin{aligned}
s_{11}'&=s_{11},\\
s_{22}'&=s_{22}\cos^4\theta+(2s_{23}+s_{44})\sin^2\theta\cos^2\theta\\
&\qquad+s_{33}\sin^4\theta,\\
s_{33}'&=s_{33}\cos^4\theta+(2s_{23}+s_{44})\sin^2\theta\cos^2\theta\\
&\qquad+s_{22}\sin^4\theta,\\
s_{44}'&=s_{44}\cos^2 2\theta+(s_{22}+s_{33}-2s_{23})\sin^2 2\theta,\\
s_{55}'&=s_{55}\cos^2\theta+s_{66}\sin^2\theta,\\
s_{66}'&=s_{66}\cos^2\theta+s_{55}\sin^2\theta,\\
s_{12}'&=s_{12}\cos^2\theta+s_{13}\sin^2\theta,\\
s_{13}'&=s_{13}\cos^2\theta+s_{12}\sin^2\theta,\\
s_{14}'&=(s_{13}-s_{12})\sin 2\theta,\\
s_{23}'&=s_{23}(\cos^4\theta+\sin^4\theta)\\
&\qquad+(s_{22}+s_{33}-s_{44})\sin^2\theta\cos^2\theta,\\
s_{24}'&=\sin^2 2\theta[(s_{23}+s_{44}/2-s_{22})\cos^2\theta\\
&\qquad+(s_{33}-s_{23}-s_{44}/2)\sin^2\theta],\\
s_{34}'&=\sin^2 2\theta[(s_{33}-s_{23}-s_{44}/2)\cos^2\theta\\
&\qquad+(s_{23}-s_{22}+s_{44}/2)\sin^2\theta],\\
s_{56}'&=(s_{55}-s_{66})\sin\theta\cos\theta.
\end{aligned} \quad (33)$$

For crystals rotated about the Y or Z axis, the constants can be obtained from these results by simply permuting the subscripts. Thus for any subscript 1, 2 or 3, 1 is added for a rotation about Y and 2 for a rotation about Z with the understanding that $3+1=1$, i.e., the subscripts rotate among themselves. The same applies to the subscripts 4, 5 and 6. For example for a rotation about Y, we have

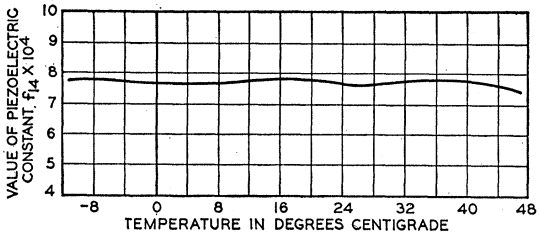

FIG. 5. A plot of the piezoelectric constant f_{14} as a function of the temperature.

$$\begin{aligned}
s_{22}'&=s_{22},\\
s_{33}'&=s_{33}\cos^4\theta+(2s_{13}+s_{55})\sin^2\theta\cos^2\theta\\
&\qquad+s_{11}\sin^4\theta, \quad (34)\\
s_{11}'&=s_{11}\cos^4\theta+(2s_{13}+s_{55})\sin^2\theta\cos^2\theta\\
&\qquad+s_{33}\sin^4\theta, \text{ etc.}
\end{aligned}$$

For a rotation about Z

$$s_{11}'=s_{11}\cos^4\theta+(2s_{12}+s_{66})\sin^2\theta\cos^2\theta+s_{22}\sin^4\theta, \text{ etc.} \quad (35)$$

We require in the text also a relation between the two piezoelectric constants e_{14} and d_{14}. From Eq. (22) we have

$$Y_z/y_z=-e_{14}/d_{14}.$$

From Eq. (1)

$$Y_z/y_z=-1/s_{44}.$$

Hence $$d_{14}=e_{14}s_{44}. \quad (36)$$

Similarly $$d_{25}=e_{25}s_{55}; \quad d_{36}=e_{36}s_{66}. \quad (37)$$

It is shown in Appendix II that in order to agree with experiment it is necessary to assume that the piezoelectric force is proportional to the charge density on the electrodes. This necessitates writing the converse piezoelectric equation in the form

$$-Y_z=f_{14}D_x; \quad -Z_x=f_{25}D_y; \quad -X_y=f_{36}D_z, \quad (38)$$

where $f_{14}=4\pi e_{14}/K_1$; $f_{25}=4\pi e_{25}/K_2$; $f_{36}=4\pi e_{36}/K_3$

and D_x, D_y and D_z are the charge densities on the electrodes perpendicular to the three axes. In these equations K_1, K_2 and K_3 are the clamped dielectric constants along the X, Y and Z axes, respectively. For the most general piezoelectric crystal we can write the inverse piezoelectric equations in the form

$$\begin{aligned}
-X_x &= f_{11}D_x + f_{21}D_y + f_{31}D_z;\\
-Y_y &= f_{12}D_x + f_{22}D_y + f_{32}D_z;\\
-Z_z &= f_{13}D_x + f_{23}D_y + f_{33}D_z;\\
-Y_z &= f_{14}D_x + f_{24}D_y + f_{34}D_z;\\
-Z_x &= f_{15}D_x + f_{25}D_y + f_{35}D_z;\\
-X_y &= f_{16}D_x + f_{26}D_y + f_{36}D_z,
\end{aligned} \tag{39}$$

where $$f_{ij} = 4\pi e_{ij}/K_i.$$

The f constants for a rotated crystal can be obtained in the same manner as the d or e constants. For example for a rotation about the X axis, the f constants transform similarly to the e constants of Eq. (31). For Rochelle salt the f_{14} constant as a function of temperature is shown plotted on Fig. 5. The f_{25} and f_{36} constants have the values

$$f_{25} = 5.17\times 10^4; \quad f_{36} = 4.81\times 10^4,$$

which are nearly independent of temperature. The f constants are much more independent of temperature and orientation than the other piezoelectric constants.

It is readily shown by reference to equations in Appendix II that for static conditions the direct and converse piezoelectric equations take the form

$$\begin{aligned}
&-P_x = e_{14}y_z; \quad -P_y = e_{25}z_x; \quad -P_z = e_{36}x_y,\\
&P_x = d_{14}Y_z; \quad P_y = d_{25}Z_x; \quad P_z = d_{36}X_y
\end{aligned} \tag{21}$$

and

$$-Y_z = f_{14}D_x; \quad -Z_x = f_{25}D_y; \quad -X_y = f_{36}D_z,$$

$$y_z = \frac{4\pi}{K_1}d_{14}D_x = \frac{d_{14}E_x}{1-k_x^2}; \quad z_x = \frac{d_{25}}{1-k_y^2}E_y; \tag{22}'$$

$$x_y = \frac{d_{36}}{1-k_z^2}E_z.$$

We note that if the usual piezoelectric Eqs. (21) and (22) are assumed valid, a larger constant d_{14} will be measured by using the converse effect than by using the direct effect if the present theory is correct. This discrepancy has been noticed experimentally,[10] but was ascribed to a lack of reversibility in Rochelle salt. On the other hand if we express the expansion and charge on the plates in terms of the applied potential and force, it is readily shown that the method of expressing the piezoelectric equations used here satisfies the reversibility law, and hence the experimental discrepancy noted receives an explanation in terms of this theory.

For dynamic conditions only the first equations of (21) and (22)′ are valid.

Appendix II

Derivation of resonant frequencies of a piezoelectric crystal

As pointed out in the introduction, the measured resonant frequencies of a longitudinally vibrating Rochelle salt crystal do not agree with those given by the usual theoretical derivation since the measured resonance and antiresonance frequencies of the plated crystal are both considerably lower than the natural resonant frequency of the crystal measured by mechanical means. It is the purpose of this appendix to give a derivation of the equation of motion of a piezoelectric crystal, whose solution agrees with the experimental results.

Let us consider a small section of a plated piezoelectric crystal cut perpendicular to the X axis and with its length 45° from the Y and Z

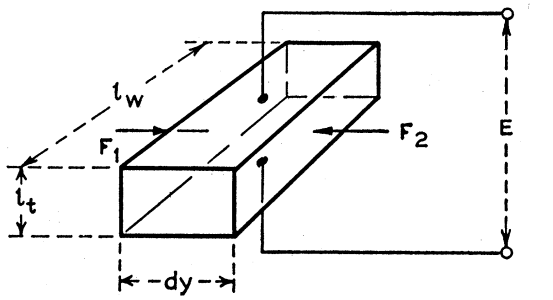

FIG. 6. A small section of a longitudinally vibrating Rochelle salt crystal.

[10] See "A Survey of Piezoelectricity," W. G. Cady, Am. Phys. Teacher **6**, 237 (1938).

axes, as shown on Fig. 6. The width of the crystal is designated by l_w, the thickness by l_t and the elementary length along the Y' axis, the direction of vibration, by dy. If we denote the displacement of the section from its equilibrium position by ξ, then by Newton's law of motion

$$\rho l_w l_t dy(\partial^2\xi/\partial t^2) = +F_1 - F_2 = -(\partial F/\partial y)dy. \quad (40)$$

Here F_1 is the compressional force exerted normal to the left surface and F_2 that normal to the right-hand surface in the direction of increasing Y'. The difference between F_1 and F_2 for the small distance dy is the derivative of F by y as indicated on the right-hand side of (40). In this equation ρ is the density of the crystal and t the time.

We next consider the force strain equation. The usual method of deriving it is as follows: If we apply a potential gradient E_x along the thickness, the piezoelectric effect will apply a force per unit area equal to

$$-Y_y' = eE_x. \quad (41)$$

This constant e is not the constant $e_{12}' = e_{14}$ of Eq. (31) of Appendix I, but the constant $d_{14}/2s_{22}'$ where s_{22}' is the inverse of Young's modulus along the length of the crystal and d_{14} the usual shear piezoelectric modulus. This fact was first pointed out by Cady[11] for quartz, and for this cut of Rochelle salt can be shown as follows. From Eq. (31) of Appendix I, we see that a field applied along the X axis excites a Y_y' and a Z_z' stress and the last through the elastic cross constants (Poisson's ratio) makes contributions to Y_y'. From the fundamental piezoelectric and elastic equations it follows that the total impressed stress causing longitudinal vibration along the crystal cut at 45° from the b and c axes is

$$-(Y_y)_1 = e_{14}\left[1 - \frac{s_{23}'}{s_{22}'}\right]E_x = \frac{e_{14}(s_{44})}{2s_{22}'}E_x = \frac{d_{14}}{2s_{22}'}E_x \quad (42)$$

upon applying the values of s' from Eq. (33) and the relation $d_{14} = e_{14}s_{44}$. The total force F is equal to $Y_y(l_w l_t)$ while the potential gradient E_x is equal to the potential E applied divided by l_t. Hence

$$-\frac{F}{l_w l_t} = \frac{d_{14}}{2s_{22}'}\frac{E}{l_t} \quad \text{or} \quad -F = \frac{d_{14}}{2s_{22}'}l_w E. \quad (43)$$

This is the force applied by the piezoelectric effect if no motion takes place. If motion takes place an additional mechanical force is applied to the section equal to

$$-\frac{l_t l_w}{s_{22}' dy}[\xi_2 - \xi_1] = -\frac{l_t l_w}{s_{22}'}\frac{\partial \xi}{\partial y}. \quad (44)$$

Hence the total force will be the sum of the piezoelectric force and the elastic force or

$$-F = \frac{l_t l_w}{s_{22}'}\frac{\partial \xi}{\partial y} + \frac{d_{14}}{2s_{22}'}El_w. \quad (45)$$

Since E the applied potential is constant for a plated crystal and is not a function of y, Eqs. (40) and (45) could be combined into

$$\frac{1}{\rho s_{22}'}\frac{\partial^2\xi}{\partial y^2} = \frac{\partial^2\xi}{dt^2} \quad (46)$$

and the electrical resonant frequency of the crystal would coincide with the natural mechanical resonant frequency of the crystal, which does not agree with the experimental results of Fig. 1.

To get an equation which agrees with experiment it is necessary to assume that the piezoelectric force of Eq. (42) is proportional to the charge density on the electrodes rather than the potential gradient. For static conditions it is obvious that Eq. (43) can be expressed in the form

$$-F = d_{14}l_w dQ/2s_{22}'C \text{ since } dQ = CE, \quad (47)$$

where dQ is the charge on the electrode elementary area $l_w dy$, and C is the capacitance of this area which is equal in c.g.s. units to

$$C = l_w dy K/4\pi l_t. \quad (48)$$

In this formula K the dielectric constant has to be the dielectric constant with the crystal clamped and prevented from moving since the force Eq. (43) is valid only for this condition.

[11] W. G. Cady, "The Piezoelectric Resonator and the Effect of Electrode Spacing Upon Frequency," Physics 7, 245 (1936).

Then Eq. (45) becomes

$$-F=\frac{l_t l_w}{s_{22}'}\frac{\partial \xi}{\partial y}+\frac{d_{14}}{2s_{22}'}\frac{4\pi l_t}{K}\frac{dQ}{dy}, \tag{49}$$

where dQ now denotes the total charge on the surface. For dynamic conditions the total derivative will be replaced by the partial so that the equation can be written

$$-F=\frac{l_t l_w}{s_{22}'}\left[\frac{\partial \xi}{\partial y}+\frac{2\pi d_{14}}{l_w K}\frac{\partial Q}{\partial y}\right]. \tag{50}$$

One farther equation connects the applied voltage to the charge generated on the surface. The total charge on the surface consists of two parts, the charge placed on the surface by the applied potential, and the charge placed on by the piezoelectric effect when the crystal expands. This total charge will then be

$$dQ=\frac{El_w dyK}{4\pi l_t}-l_w dy e_{14}(y_y'-z_z') \tag{51}$$

by virtue of the piezoelectric relation (30) of Appendix I. But for a longitudinal vibration along Y', $z_z'=(s_{23}'/s_{22}')y_y'$ since s_{23}'/s_{22}' is Poisson's ratio by virtue of Eq. (1). Eq. (51) then becomes

$$dQ=\frac{l_w dyK}{4\pi}\left[\frac{E}{l_t}-\frac{4\pi d_{14}}{2s_{22}'K}\frac{\partial \xi}{\partial y}\right], \tag{52}$$

taking account of the relations given in Eq. (43), and the fact that $y_y'=\partial\xi/\partial y$.

For an unconstrained crystal F of Eq. (49) is zero so that

$$\frac{\partial \xi}{\partial y}=-\frac{4\pi d_{14}}{2l_w K}\frac{dQ}{dy}.$$

Substituting in (52) we find

$$C_F=\frac{dQ}{E}=\frac{Kl_w dy}{4\pi l_t(1-k^2)}, \tag{53}$$

where the coupling k is defined by the equation

$$k=\frac{d_{14}}{2}\left(\frac{4\pi}{Ks_{22}'}\right)^{\frac{1}{2}}. \tag{54}$$

Eq. (53) shows that the dielectric constant of a crystal free to move is related to the dielectric constant of a clamped crystal by

$$K_F=K/(1-k^2). \tag{55}$$

For dynamic conditions, Eq. (52) can be written

$$\frac{\partial Q}{\partial y}=\frac{l_w K}{4\pi}\left[\frac{E}{l_t}-\frac{4\pi d_{14}}{2s_{22}'K}\frac{\partial \xi}{\partial y}\right]. \tag{56}$$

Eqs. (40), (50) and (56) give sufficient data to solve the problem. They are collected together in one equation for reference.

$$\rho l_w l_t dy\frac{\partial^2 \xi}{\partial t^2}=F_1-F_2=\frac{-\partial F}{\partial y}dy, \quad \text{(A)}$$

$$-F=\frac{l_t l_w}{s_{22}'}\left[\frac{\partial \xi}{\partial y}+\frac{2\pi d_{14}}{l_w K}\frac{\partial Q}{\partial y}\right], \quad \text{(B)} \tag{57}$$

$$\frac{\partial Q}{\partial y}=\frac{l_w K}{4\pi}\left[\frac{E}{l_t}-\frac{4\pi d_{14}}{2Ks_{22}'}\frac{\partial \xi}{\partial y}\right]. \quad \text{(C)}$$

Differentiating (57B) with respect to y and substituting the result in Eq. (57A) we have

$$\rho\frac{\partial^2 \xi}{\partial y^2}=\frac{1}{s_{22}'}\left[\frac{\partial^2 \xi}{\partial y^2}+\frac{4\pi d_{14}}{2l_w K}\frac{\partial^2 Q}{\partial y^2}\right]. \tag{58}$$

For a plated crystal E the applied potential is constant along the crystal and hence is not a function of y. Differentiating (57C) by y we have

$$\frac{\partial^2 Q}{\partial y^2}=-\frac{d_{14}}{2s_{22}'}l_w\frac{\partial^2 \xi}{\partial y^2},$$

which simplifies (58) to the form

$$\rho\frac{\partial^2 \xi}{\partial t^2}=\frac{(1-k^2)}{s_{22}'}\frac{\partial^2 \xi}{\partial y^2}. \tag{59}$$

For simple harmonic motion, (59) is satisfied by the relation

$$\xi=A\cos\frac{\omega}{v'}y+B\sin\frac{\omega}{v'}y \tag{60}$$

where $v'=((1-k^2)/\rho s_{22}')^{\frac{1}{2}}$.

When $y=0$, $A=\xi_1$ the displacement at the point $y=0$. Differentiating ξ by y we have

$$\frac{\partial \xi}{\partial y}=-A\frac{\omega}{v'}\sin\frac{\omega}{v'}y+B\frac{\omega}{v'}\cos\frac{\omega}{v'}y.$$

Hence

$$B=\left(\frac{\partial \xi}{\partial y}\right)_1\frac{v'}{\omega}.$$

Solving (57B) and (57C) simultaneously for $\partial\xi/\partial y$ we find

$$-\frac{\partial\xi}{\partial y}=\frac{s_{22}'}{l_t l_w(1-k^2)}\left[F+\frac{d_{14}}{2s_{22}'}l_wE\right]. \quad (61)$$

Inserting these values of A and B in (60), we have

$$\xi=\xi_1\cos\frac{\omega}{v'}y-\frac{[F_1+(d_{14}/2s_{22}')l_wE]}{l_t l_w\omega(\rho(1-k^2)/s_{22}')^{\frac{1}{2}}}\sin\frac{\omega}{v'}y. \quad (62)$$

From (60) and (61) we have also the relation

$$\left(F+\frac{d_{14}}{2s_{22}'}l_wE\right)=\left(F_1+\frac{d_{14}}{2s_{22}'}l_wE\right)\cos\frac{\omega}{v'}+\xi_1\omega l_t l_w\left(\frac{\rho(1-k^2)}{s_{22}'}\right)^{\frac{1}{2}}\sin\frac{\omega y}{v'}. \quad (63)$$

A third relation can be obtained by integrating (57C) directly. Since E is independent of y, we have

$$Q=\frac{l_w l_y KE}{4\pi l_t}-\frac{d_{14}l_w}{2s_{22}'}(\xi_2-\xi_1), \quad (64)$$

where l_y is the length of the crystal along the direction of vibration, and ξ_2 and ξ_1 are the displacements on the two ends of the crystal.

These three equations, which will determine the impedance of a crystal for any mechanical terminating conditions, are gathered together as Eq. (65). In this equation, however, we have replaced the particle displacement by the particle velocity and the charge by the current which can be done for simple harmonic motion by dividing the displacement and charge by $j\omega$. We have then

$$\dot{\xi}=\dot{\xi}_1\cos\frac{\omega}{v'}y-\frac{j[F_1+(d_{14}/2s_{22}')l_wE]}{l_t l_w(\rho(1-k^2)/s_{22}')^{\frac{1}{2}}}\sin\frac{\omega}{v'}y \quad (A)$$

$$\left[F+\frac{d_{14}}{2s_{22}'}l_wE\right]=\left(F_1+\frac{d_{14}l_w}{2s_{22}'}E\right)\cos\frac{\omega}{v'}y-j\dot{\xi}_1 l_t l_w\left(\frac{\rho(1-k^2)}{s_{22}'}\right)^{\frac{1}{2}}\sin\frac{\omega y}{v'} \quad (B) \quad (65)$$

$$E(j\omega C_0)=i+\frac{d_{14}l_w}{2s_{22}'}(\dot{\xi}_2-\dot{\xi}_1), \quad (C)$$

where C_0 is the total capacity of the crystal clamped, i.e., $(Kl_w l_y/4\pi l_t)$. These equations are of interest for supersonic phenomena as well as to determine the impedance of a crystal element. An example is considered later.

For a freely vibrating crystal, the forces on the two ends are zero. Introducing these values in (65A) and (B) we find

$$\dot{\xi}_1=-\dot{\xi}_2=\frac{jd_{14}E(1-\cos\omega l_y/v')}{2l_t(\rho s_{22}'(1-k^2))^{\frac{1}{2}}\sin\omega l_y/v'}=\frac{jd_{14}E}{2l_t(\rho s_{22}'(1-k^2))^{\frac{1}{2}}}\tan\frac{\omega l_y}{2v'}. \quad (66)$$

Inserting these values in Eq. (65C) and solving for the ratio of E/i, we find the impedance of the crystal to be

$$Z_C=\frac{E}{i}=\frac{-j}{\omega C_0\left[1+\dfrac{[k^2/(1-k^2)]}{\omega l_y/2v'}\tan\dfrac{\omega l_y}{2v'}\right]}. \quad (67)$$

The first electrical resonance will occur when

$$\tan\frac{\omega l_y}{2v'}=\infty \quad \text{or} \quad f_R=\frac{1}{2l_y}\left(\frac{(1-k^2)}{\rho s_{22}'}\right)^{\frac{1}{2}}. \quad (68)$$

This is lower than the natural mechanical resonance of the crystal by the factor $(1-k^2)^{\frac{1}{2}}$ in agreement with the experimental data of Fig. 1. When the denominator is zero, the impedance will be infinite and an antiresonance will occur. The frequency of antiresonance is given by the formula

$$\frac{\omega l_y}{2v'}\cot\frac{\omega l_y}{2v'}=-\frac{k^2}{1-k^2}. \quad (69)$$

Fig. 7 shows the calculated resonant and antiresonant frequencies plotted as a ratio to the natural mechanical resonant frequency for a given electromechanical coupling. It will be noted that both the resonant and antiresonant frequencies are lower than the natural mechanical

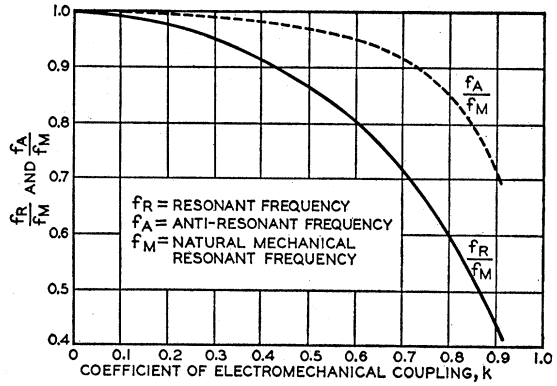

FIG. 7. Theoretical curves showing, respectively, the ratio between the electrical resonant and the natural mechanical resonant frequencies and the ratio between the electrical antiresonant frequency and the natural mechanical resonant frequency plotted as a function of the electromechanical coupling.

resonance of the crystal by considerable amounts when the coupling is large. Comparing the ratio of antiresonance to resonance for the measured curves of Fig. 1 and the theoretical curves of Fig. 7, the coupling can be evaluated for a Rochelle salt crystal as a function of temperature. This curve is plotted on Fig. 2. Knowing the coupling the natural mechanical resonant frequency can be calculated from Eq. (68). A calculation of this quantity for the crystal of Fig. 1 is shown by the dot-dash line labeled *D* of Fig. 1. This is slightly lower than that measured in an air-gap holder, but agrees in shape very well with that curve. The slight lowering is probably due to the weight of the plating used to drive the crystal. Hence the theory presented here agrees very well with the measured results.

In the introduction it was shown experimentally that the measured resonance and antiresonance frequency of a crystal approached the natural mechanical resonance frequency when the amount of plating was small. This can be proved theoretically by the use of Eqs. (65). We consider first the case of a crystal cemented on its two ends to two identical bars which it drives in longitudinal motion. Assuming that the cement is very thin and stiff, so that its mechanical impedance can be neglected, the crystal will drive two bars free on one end whose mechanical impedances are known to be[12]

$$Z_M = jZ_0 \tan \omega l_1/v_1, \quad \text{where} \quad Z_0 = l_{t_1} l_{w_1} \rho_1 v_1. \tag{70}$$

In this equation l_{t_1} is the thickness of the bars, l_{w_1} their width, and l_1 their length (measured in centimeters), ρ_1 the density and v_1 the velocity of propagation in the attached bars. Since this is the mechanical impedance that the crystal is terminated in on each side, we have the termination conditions

$$\frac{F_2}{\dot{\xi}_2} = \frac{-F_1}{\dot{\xi}_1} = jZ_0 \tan \frac{\omega l_1}{v_1}. \tag{71}$$

The negative sign arises since the ratio of force to velocity for the assumed directions are opposite for the two ends.

Inserting these ratios in Eqs. (65A) and (65B) and solving for the electrical impedance from (65C) we find

$$Z = \frac{E}{i} = \frac{-j}{\omega C_0 \left[1 + \frac{[k^2/(1-k^2)]}{\omega l_y/2v'} \left(\frac{\tan \omega l_y/2v'}{1 - Z_0/Z_0' \tan \omega l_y/2v' \tan \omega l_1/v_1} \right) \right]}, \tag{72}$$

where Z_0' is the mechanical impedance of the crystal, i.e., $l_t l_w \rho v'$. The resonant frequencies of the combination are given by

$$\tan \frac{\omega l_y}{2v'} \tan \frac{\omega l_1}{v_1} = \frac{Z_0'}{Z_0} = \frac{l_t l_w \rho v'}{l_{t_1} l_{w_1} \rho_1 v_1}, \tag{73}$$

while the antiresonant frequencies are given by the equation

$$\cot \frac{\omega l_y}{2v'} - \frac{Z_0}{Z_0'} \tan \frac{\omega l_1}{v_1} = -\left[\frac{k^2/(1-k^2)}{\omega l_y/2v'} \right]. \tag{74}$$

TABLE IV.

PERCENT PLATING	f_R/f_M	f_A/f_M	r CALCULATED
100	0.9951	0.99910	124.5
80	.99523	.99978	109.0
60	.99562	1.0000	113.3
40	.99663	1.0000	143.0
20	.99810	1.0000	262.0
0	1.0000	1.0000	∞

[12] This is easily proved from (65B) by letting d_{t_4} and hence $k=0$ and setting $F_2=0$. The result is $F_1/\dot{\xi}_1 = jZ_0 \tan \omega l_1/v_1$ where $Z_0 = l_t l_w (\rho/s_{22}')^{\frac{1}{2}}$, $v_1 = (1/\rho s_{22}')^{\frac{1}{2}}$.

The case of interest is the case where the crystal is only partially plated in such a manner that a certain percentage of the length on each end is left unplated. For this case the cross-sectional area is constant down the whole length and the ratio

$$Z_0'/Z_0=(1-k^2)^{\frac{1}{2}}. \tag{75}$$

For X cut quartz crystals for example with their lengths along the Y or mechanical axis, the value of k has been found to be 0.099. A calculation was made of the ratio of the resonant frequency to the natural mechanical resonant frequency for various percentages of the crystal plated and the results are shown in Table IV.

This table shows also the ratio of the antiresonant frequency to the natural mechanical resonant frequency of the crystal while the third column gives the ratios of capacitances C_2 to C_1 in the equivalent electrical circuit of the crystal shown on Fig. 8. It is obvious that the crystal is most efficiently driven when it is about 70 percent plated, and this deduction has been verified experimentally.[13] The same conclusions hold for any other type of piezoelectric crystal. It will be noted that when the percent of plating becomes small both the resonant and antiresonant frequencies approach the natural mechanical resonant frequency f_m. The antiresonant frequency agrees with f_m when the amount of plating is 50 percent or less.

Another question of importance which can easily be solved by this method is the effect of an air gap between the crystal and the driving plates on the frequency of the crystal. The method of deriving the equations is the same as above, except that we have to calculate what part of the total potential is applied across the crystal and what part in the air gap. Eqs. (57)

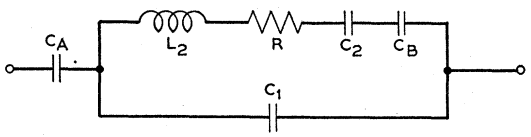

FIG. 8. An electrical circuit representing the electrical impedance of a piezoelectric crystal.

[13] This result was first shown experimentally by Mr. R. A. Sykes.

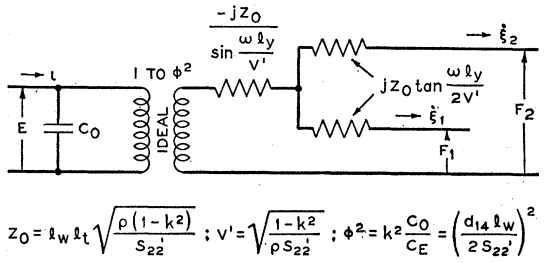

FIG. 9A

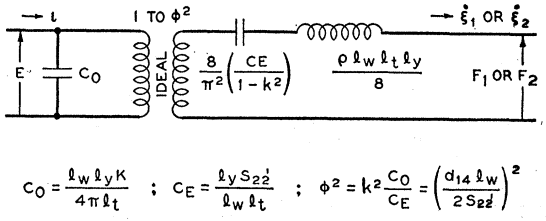

FIG. 9B

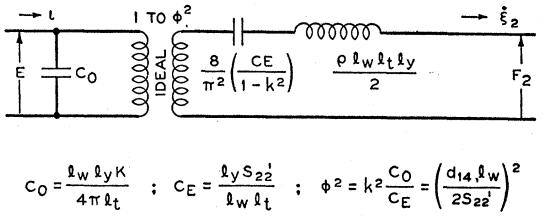

FIG. 9C

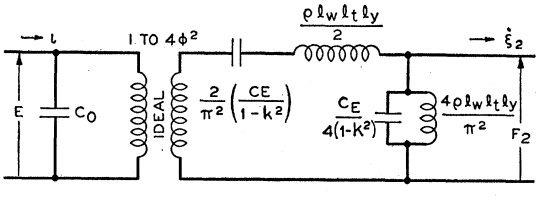

FIG. 9D

FIG. 9. An electromechanical representation of a piezoelectric crystal. (A) An exact representation, (B) a lumped constant representation for a symmetrical crystal, (C) a lumped constant representation for a crystal clamped on one end, (D) a lumped constant representation for a crystal free on one end and driving a load on the other.

become

$$\rho l_w l_t dy(\partial^2\xi/\partial t^2)=(-\partial F/\partial y) \quad \text{(A)}$$

$$-F=\frac{l_t l_w}{s_{22}'}\left[\frac{\partial\xi}{\partial y}+\frac{4\pi d_{14}}{2Kl_w}\frac{\partial Q}{\partial y}\right], \quad \text{(B)} \qquad (76)$$

$$\frac{\partial Q}{\partial y}=\frac{l_w l_t K}{4\pi(Kl_A+l_t)}\left[\frac{E}{l_t}-\frac{4\pi d_{14}}{2Ks_{22}'}\frac{\partial\xi}{\partial y}\right], \quad \text{(C)}$$

where l_A is the total air gap on both sides of the crystal, and Q the charge on the elementary section of the plating. The solution for the impedance of the crystal becomes

$$Z_c=\frac{-j}{\omega C_0'\left[1+\dfrac{[k'^2/(1-k'^2)]\tan\omega l_y/2v''}{\omega l_y/2v''}\right]}, \qquad (77)$$

where $$C_0'=\frac{Kl_w l_y}{4\pi(Kl_A+l_t)};$$

$$k'^2=\left(\frac{l_t}{Kl_A+l_t}\right)\frac{4\pi(d_{14}/2)^2}{Ks_{22}'};$$

$$v''=((1-k'^2)/\rho s_{22}')^{\frac{1}{2}}.$$

Hence the effect of an air gap is to change the static capacitance and the square of the electromechanical coupling by the factor $l_t/(Kl_A+l_t)$. In the limiting case when l_A becomes large, the coupling k' approaches zero and hence the measured resonance of the crystal will approach the natural mechanical resonance of the crystal. It is, therefore, valid to measure the elastic constants as described above in an air-gap holder.

An equivalent electrical circuit which will represent the impedance of Eq. (77) in the neighborhood of the resonant and antiresonant frequencies is shown on Fig. 8. These elements have the values

$$C_1=\frac{Kl_w l_y}{4\pi l_t};\quad C_2=\frac{8k^2C_1}{\pi^2(1-k^2)};$$
$$C_A=\frac{l_w l_y}{4\pi l_A};\quad C_B=\frac{8(C_1+C_A)}{\pi^2-8};\quad L_2=\frac{s_{22}'\rho l_y^2}{8k^2C_1}. \qquad (78)$$

The resistance shown represents the dissipation put in by internal losses, clamping losses, and all other sources.

An exact electromechanical representation[14] of a plated piezoelectric crystal is shown on Fig. 9(A). If one solves for the equations of this network, they reduce to those given by Eqs. (65). If we only wish to use the representation near the resonant frequency, lumped network representations can be used. Fig. 9(B) shows a representation for a symmetrical crystal driving equal loads on each end. Fig. 9(C) shows a representation for a crystal clamped on one end and driving a load on the other end, while Fig. 9(D) shows a representation for a crystal free on one end and driving a load on the other (inertia drive).

[14] An approximate representation is discussed in a previous paper "An Electro-mechanical Representation of a Piezo-Electric Crystal used as a Transducer," W. P. Mason, Proc. I. R. E. **23**, 1252 (1935).